Noise analysis of a resonance sensor platform for enhanced limit of detection

W.A.P.M. Hendriks, J.P. Korterik, M. de Goede, M. Dijkstra and Sonia M. Garcia-Blanco

MESA+ Institute, University of Twente, P.O. Box 217, 7550 AE, Enschede, The Netherlands

Resonance sensors have been shown to be highly sensitive [1], [2]. *Their performance is however limited by the presence of noise in the signal amplitude and the resonance position of the resonator* [3]. *We will analyze the effects of the noise sources in our setup and the performance increase that can be achieved using several resonant sensor configurations. Finally, we will show the achieved increase in limit of detection for the optimized system.*

Introduction

Optical resonance sensors have been of interest for label free biomarker sensing for decades. Different approaches for integrated optical biosensors have been shown, such as surface plasmon resonance (SPR)[4], interferometers[5] and resonance sensors such as photonic crystal cavities or micro ring resonators (MRR)[1], [6].
In recent years, MRR sensors have matured to the level of commercially viable products[7]. The performance of these sensors is still far away from their theoretical intrinsic limit of detection defined as,

$$LOD_{intrinsic} = \frac{\Delta\lambda}{S}$$

where $\Delta\lambda$ is the resonance linewidth and S is the sensitivity indicating the observed resonance shift per change in refractive index unit (RIU). MRR sensors can be designed to have low $LOD_{intrinsic}$ due to the narrow resonance features of the MRR, which are a consequence of the low loss waveguide platform in which they can be fabricated. The narrow resonances allow for very accurate determination of resonance shift. The performance of the sensors is however limited by noise sources influencing the resonance position. As a result the resonance position changes over time limiting the measured limit of detection (LOD). The LOD is then determined by the noise floor of the sensors and the sensitivity of the sensor defined as,

$$LOD = \frac{3\sigma}{S}$$

where 3σ is the 98% confidence interval of the sensor response without a signal of interest present and S is the sensitivity of the sensor. There is a lot of interest in increasing the sensitivity of the MRR sensors [8]. However as an increased sensitivity simultaneously leads to a higher noise floor, due to thermal noise, this does not improve the actual limit of detection[3]. The increase in sensitivity of these resonators therefore only results in an improved LOD when the noise can be sufficiently limited.
For this reason we will investigate several strategies to limit the noise floor. The analysis will be based on the Al_2O_3 MRR platform as described by M. de Goede et. al. [1]. The results found for this particular system can be generalized to apply to other resonance sensors and interferometers for as long as the setup is based on a tunable laser source and detector to investigate the wavelength shift.

Noise sources description

The model system consists of a tunable laser with a single MRR and a photodetector with readout electronics. For this model system three distinct noise terms can be distinguished. The first is the spectral deviation $\sigma_{spectral}$, from other sources then the signal of interest. The second noise term is the peak position determination error introduced by amplitude variations $\sigma_{amplitude}$. The amplitude variations are introduced by the tunable laser power instability and the amplitude noise in the photodetector and readout electronics or even drift in the alignment. Finally, the temperature instability of the sample stage and therefore the MRR will introduce a temperature dependent noise term $\sigma_{temperature}$. The total system noise can then be found by summing the individual noise variances.

$$3\sigma = 3\sqrt{\sigma_{spectral}^2 + \sigma_{amplitude}^2 + \sigma_{temperature}^2}.$$

To reduce the noise on the system we will investigate each term to determine its influence and how to reduce it.

Spectral noise

The first source to consider is the spectral noise in the system, for which two distinct sources of error in wavelength determination can be distinguished. Consider a case in which the tunable laser source starts scanning at some wavelength, $\lambda_{initial}$, and stops the scan at λ_{final}. The first source of inaccuracy in determining the correct wavelength at every data point is the inaccuracy in the relative change between each data point. The second inaccuracy is the relative difference between scans for the start and stop wavelength. Both terms can be significantly reduced by implementing an interferometer to simultaneously measure the wavelength scan. Scanning in one direction and counting the interferometer fringes gives an inaccuracy determined by the free spectral range (FSR) of the interferometer and the sampling rate of the detector. If this principle is extended to measuring both in the forward and backwards direction of the scan, the accuracy can be extended to eliminate the inaccuracy of the initial starting wavelength for the scans as this will reduce to an absolute error on the entire measurement. We then end up with an relative inaccuracy in the wavelength for a general system that is determined by the number of data points in one period of the interferometer

$$\Delta\lambda = \frac{scanspeed}{sa\ mple\ rate}.$$

This is reasonable as long as the FSR of the interferometer is not much larger than $\Delta\lambda$.

Amplitude noise

The second noise source is determined by the inaccuracy in the fit that occurs because of the variations in the amplitude on the ring spectrum. To determine this influence, we generate a Lorentzian waveform to which Gaussian noise is added with different signal to noise ratios. This influence is modeled for FWHM values of the Lorentzian curve corresponding to Q values from ten thousand up to ten million. This limitation is chosen as resonance positions for lower Q values are more accurately determined using an FFT method[9]. The upper limit is chosen as it approaches the attainable limit for resonators in water at 1550 nm. Finally jitter in the peak position of 10 times the FWHM is added, to ensure the initial guess for the fitting is not the actual optimum. Increasing this value further did not have any significant influence on the found variance. The generated

Lorentzian dip is fitted using the Matlab least square fitting algorithm with the Lorentzian defined as

$$L(x) = a - \frac{1}{\pi}\frac{\frac{1}{2}\Gamma}{(x-x_0)^2 + \left(\frac{1}{2}\Gamma\right)^2},$$

Where Γ indicates the FWHM of the function and x_0 is the center position. For this function four free parameters for the fit can be defined, the center frequency x_0, the off resonance amplitude a and two variables containing the FWHM $\frac{\Gamma}{2\pi}, \left(\frac{1}{2}\Gamma\right)^2$. For this model the variance on the fit is found to be below 0.1 pm for even the SNR of 10dB or 10%. For the model system of [1] this would correspond to a contribution on the noise floor of $\sigma_{amplitude} = 10^{-2} pm$.

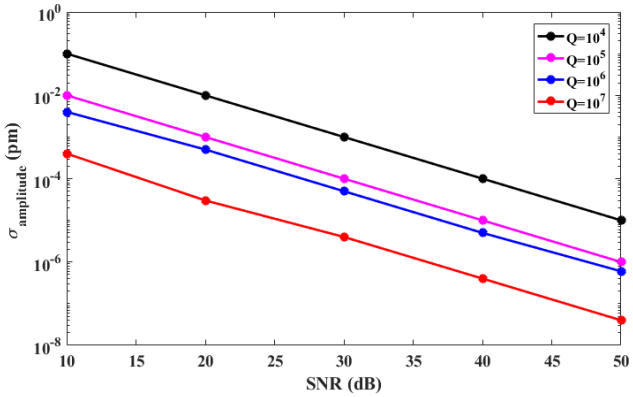

Figure 1 Variance on the found peak position for a least square fit of a Lorentzian with added noise, where the signal to noise ratio SNR is defined as defined the normalized signal amplitude divided by the variance of the noise

Temperature noise

The final noise term to characterize is the temperature variation on the chip. From a variational treatment of the perturbations due to temperature induced refractive index changes, we can express the variation in resonance position as a function of the variance of the sample temperature $\Delta\sigma_T(\lambda)$. [10]–[12],

$$\Delta\sigma_{temperature}(\lambda) = \frac{2 \cdot \lambda_{\text{resonance}} \cdot c \cdot \Delta\sigma_{temperature}(T)(\sum_i n_i \left(\frac{dn}{dt}\right)_i \langle \boldsymbol{e}|\boldsymbol{e}\rangle_i)}{n_{group}}$$

Where $\Delta\sigma_{temperature}(T)$ is the standard deviation drift of the temperature, c is the speed of light, the subscript indicates the different materials of the waveguide cross sections and **e** is the transversal electric field of the fundamental mode, which is integrated over the cross-sectional area with the bounds of the material. It is thus the electric field intensity overlap with a material.

The thermo-optic coefficients for water and SiO_2 at a wavelength of 1550 nm can be found to be $-85 \cdot 10^{-6}[K^{-1}]$ and $9.5 \cdot 10^{-6}[K^{-1}]$ respectively [13], [14].

The thermo-optic coefficient for Al_2O_3 is found to be in the order of $1 \cdot 10^{-5}[K^{-1}]$[15]. As the thermo-optic coefficient of water is negative, in principle it should be possible to design a waveguide that cancels the total waveguide thermo-optic coefficient. However, as there is an order of magnitude difference between the thermo-optic coefficients, this a

very instable optimum. Therefore, the temperature sensitivity of the Al_2O_3 sensor platform is a given as long as the field is primarily confined in the core and substrate. The performance can thus be significantly improved by accurately controlling the sample temperature. We compare two cases, the first being an PID controlled temperature stage as used in [1], using heating resistors on the sample holder, which result in temperature stability of $\sigma_T(T) = 10\ mK$ and a noise contribution of $\sigma_T(\lambda) = 10^{-1}\ pm$. Placing the sample and holder in an enclosure, a temperature stability $\sigma_T(T) = 1\ mK$ is obtained. For the enclosed case we find a temperature contribution on the noise in the order of $\sigma_T(\lambda) = 10^{-2} pm$.

Conclusion

For the model system considered we find that the system noise floor contributions can be reduced. The amplitude noise influence on the fitting for the MRR is found to be below $10^{-2} pm$, which is an order of magnitude below the reported variance of the total system. The variance on the laser wavelength, can be improved by implementing an interferometer along with the tunable laser reducing the variance on the wavelength to $10^{-2} pm$ for an 1m path length difference. Finally putting an enclosure around the setup improves the final variance to $10^{-2} pm$, for the model system with a sensitivity of 100nm/RIU this would correspond to a LOD improvement from 10^{-6}. to 10^{-7}.

References

[1] M. de Goede, M. Dijkstra, R. O. Núñez, E. Martínez, and S. M. García-Blanco, "High quality factor Al_2O_3 microring resonators for on-chip sensing applications," vol. 10535, p. 1053504, Feb. 2018.

[2] M. Iqbal *et al.*, "Label-free biosensor arrays based on silicon ring resonators and high-speed optical scanning instrumentation," *IEEE J. Sel. Top. Quantum Electron.*, vol. 16, no. 3, pp. 654–661, 2010.

[3] I. M. White and X. Fan, "On the performance quantification of resonant refractive index sensors," *Opt. Express*, vol. 16, no. 2, p. 1020, Jan. 2008.

[4] H. Vaisocherová, "SPR biosensors for medical diagnostics," in *Engineering*, no. July, 2006, pp. 229–247.

[5] T. Chalyan *et al.*, "Asymmetric mach-zehnder interferometer based biosensors for aflatoxin M1 detection.," *Biosensors*, vol. 6, no. 1, Jan. 2016.

[6] H. Inan *et al.*, "Photonic crystals: emerging biosensors and their promise for point-of-care applications.," *Chem. Soc. Rev.*, vol. 46, no. 2, pp. 366–388, Jan. 2017.

[7] S. Mudumba *et al.*, "Photonic ring resonance is a versatile platform for performing multiplex immunoassays in real time," *J. Immunol. Methods*, vol. 448, pp. 34–43, Sep. 2017.

[8] X. Sun, D. Dai, L. Thylén, and L. Wosinski, "Double-slot hybrid plasmonic ring resonator used for optical sensors and modulators," *Photonics*, vol. 2, no. 4, pp. 1116–1130, Nov. 2015.

[9] L. Gounaridis *et al.*, "High performance refractive index sensor based on low Q-factor ring resonators and FFT processing of wavelength scanning data," *Opt. Express*, vol. 25, no. 7, p. 7483, Apr. 2017.

[10] H. A. Haus, Waves and fields in optoelectronics TT -. Englewood Cliffs, NJ : Prentice-Hall.

[11] D. L. Lee, Electromagnetic principles of integrated optics TT -. New York : Wiley.

[12] W. Bogaerts *et al.*, "Silicon microring resonators," *Laser and Photonics Reviews*, vol. 6, no. 1. WILEY-VCH Verlag, pp. 47–73, 02-Jan-2012.

[13] A. W. Elshaari, I. E. Zadeh, K. D. Jons, and V. Zwiller, "Thermo-optic characterization of silicon nitride resonators for cryogenic photonic circuits," *IEEE Photonics J.*, vol. 8, no. 3, pp. 1–9, Jun. 2016.

[14] Y. Ho Kim *et al.*, "Thermo-optic coefficient measurement of liquids based on simultaneous temperature and refractive index sensing capability of a two-mode fiber interferometric probe," vol. 18, no. 22, pp. 1973–1975, 1993.

[15] C. C. Kores, N. Ismail, D. Geskus, M. Dijkstra, E. H. Bernhardi, and M. Pollnau, "Temperature dependence of the spectral characteristics of distributed-feedback resonators," *Opt. Express*, vol. 26, no. 4, p. 4892, Feb. 2018.